ACTA ACUSTICA UNITED WITH ACUSTICA
Vol. 95 (2009) 379 – 385

DOI 10.3813/AAA.918160

Two Listeners Crosstalk Cancellation System Modelled by Four Point Sources and Two Rigid Spheres

Bruno Masiero
Institute of Technical Acoustics, RWTH Aachen University, 52056 Aachen, Germany.
bma@akustik.rwth-aachen.de

Xiaojun Qiu
Institute of Acoustics, Nanjing University, China

Summary
In virtual acoustic imaging systems, the perception of a sound source anywhere in space can theoretically be reproduced for one listener by using only two loudspeaker and an appropriate set of filters, called *crosstalk cancellation* (CTC) filters. However, the ideal position of the loudspeakers in such systems is still a question that is currently addressed by many researchers. Several analytical models with varying degrees of complexity have been used to analyze this matter. The fact is that, so far, all implemented CTC systems were built for a single listener use. When it comes to two listener CTC systems, the conditioning of the matrix of transfer functions between the loudspeakers and the listener's ear seems to be more irregular than the conditioning of the matrix for a one listener CTC system. Using a simplified model made it possible to verify that the position of the sound sources also plays a major role as far as the two listeners system's performance is concerned. Now, the influence of the presence of the listener's head in this model is evaluated. The free-field model of a two listener CTC system is expanded by modelling the listeners' heads as two rigid spheres. Using this new model an optimal source displacement is calculated based on two potential source distribution arrangements, namely a linear and a circular source distribution.

PACS no. 43.38.Md, 43.60.Dh, 43.60.Tj

1. Introduction

Given the advances in the field of acoustic virtual reality, it is now possible to simulate the noise of an automobile or a household appliance, or even to predict how a certain room (especially expensive concert halls) will sound like [1]. These simulations are generally based on the binaural hearing. The term binaural hearing refers to the fact that the human brain can detect the position of a sound source with the help of the small spectral differences between the sound heard on the left and right ears. All calculations are aimed at generating sound signals that *one* listener would hear if he or she were inside the simulated room or near the simulated noise source.

Of course the same binaural signal could be played simultaneously for many listeners, each of whom using its own headphones. But they would all have the same acoustical excitation, which would probably not match their individual visual excitation. That means that it is necessary to calculate an independent binaural signal for each user in a multi-user virtual reality environment, and that each signal has to be later played through individual headphones.

For some applications, such as psychometric or comfort tests, the use of headphones might be unsuitable. The *crosstalk cancellation* technique is usually applied to reproduce a binaural signal using a pair of loudspeakers [2, 3, 4]. This technique requires a set of filters to mix both channels of the binaural signal so that after playback, the left ear will only hear the desired left channel and the right ear only the right channel. The transfer function between loudspeakers and listener's ears is required to design the ideal set of filters for a CTC system. This transfer functions are commonly known as *head related transfer functions* (HRTFs) and are usually measured using dummy heads.

For a theoretical analysis of the CTC system, the HRTFs are calculated based on an analytical model of the virtual imaging reproduction system. The first analysis of this kind involved a free-field model. The two loudspeakers used for this model were modelled as two spherical point sources while the listener was modelled as two point receivers representing the listeners ears [2, 5, 6]. Nelson and Rose later expanded this model and placed a rigid sphere between the point receivers to account for the diffraction

Received 30 May 2008,
accepted 20 November 2008.

effect of the listener's head [7]. HRTFs calculated with the rigid sphere model conform better to measured HRTFs than the HRTFs calculated with the free-field model. Nelson and Rose verified that the presence of a rigid sphere reduces the peaks in the transfer matrix condition number. However, the basic dependence of condition number on the loudspeaker position and the frequency remains very similar to that predicted by the free-field model. They conclude by suggesting that different loudspeaker arrangements should be used in different frequency ranges in order to keep the inversion problem well conditioned.

At present, research in the field of multi-listeners acoustic virtual reality environments concentrate on the wave field reproduction approach, being *high order Ambisonics* (HOA) and *wave field synthesis* (WFS) the two main reproduction schemes of that kind. This approach makes it possible to reproduce the sound field of an entire desired virtual location inside a delimited listening area, instead of reproducing the sound field only at the position of the listeners' ears [8, 9]. Bauck and Cooper proved that the expansion of a CTC system for multiple users was mathematically feasible [10]. Later Kim *et al.* published the first simulations involving a two listeners CTC system [11]. They tried to optimize the sound source arrangement as to minimize the condition number of the systems transfer matrix allowing the construction of more stable filter sets.

In this paper an improved model for the two listener CTC system is proposed, which models the heads of the two listeners as two rigid spheres. This new model makes it possible to take phenomena such as wave diffraction and interaction between diffraction from both spheres into account. It provides an estimate of the HRTF set of a listener with the presence of another listener in its vicinity, allowing, therefore, a more realistic analysis of the two listeners CTC system. The two rigid sphere model is presented in section 2. In section 3 the results of simulations with the proposed model is discussed and afterwards two different source distributions schemes are analyzed.

2. Analytical model

The geometry of the problem discussed in this paper is shown in Figure 1. Two rigid spheres are used to approximate the listeners' heads. Each sphere has its own spherical coordinate system, referred to as O_1 and O_2. A monopole point source is located at $\boldsymbol{r}_{1s} = (r_{1s}, \theta_{1s}, \phi_{1s})$ in the coordinate system O_1 or at $\boldsymbol{r}_{2s} = (r_{2s}, \theta_{2s}, \phi_{2s})$ in the coordinate system O_2. A receiver point is located at $\boldsymbol{r}_{1r} = (r_{1r}, \theta_{1r}, \phi_{1r})$ in the coordinate system O_1 or at $\boldsymbol{r}_{2r} = (r_{2r}, \theta_{2r}, \phi_{2r})$ in the coordinate system O_2. The XZ planes of both coordinate systems are located within the same plane and in the same direction, and therefore $\phi_1 = \phi_2$. The total sound field that is created around the two spheres and that is irradiated by a point source in a free field consists of three parts: the primary incident field, the scattered field from Sphere 1, and the scattered field from Sphere 2; and can be expressed as

$$p_t(\boldsymbol{r}) = p_p(\boldsymbol{r}) + p_{s_1}(\boldsymbol{r}) + p_{s_2}(\boldsymbol{r}). \quad (1)$$

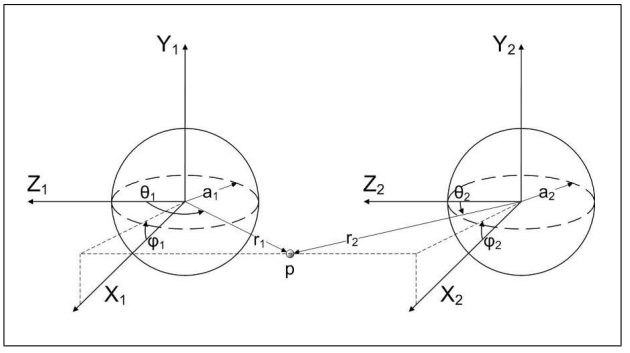

Figure 1. The free field geometrical arrangements of a point with two rigid spheres.

The primary incident field generated by a point source in free space, without any scattering objects, can be expanded in terms of spherical harmonics [12, 13] as

$$p_p(\boldsymbol{r}) = \mathrm{i}P_0 \frac{\mathrm{e}^{-\mathrm{i}k|\boldsymbol{r}|}}{|\boldsymbol{r}|} = 4\pi k P_0 \cdot \sum_{l=0}^{\infty} \left[j_l(kr_<) h_l(kr_>) \sum_{m=-l}^{l} Y_{lm}^*(\theta_s, \phi_s) Y_{lm}(\theta_r, \phi_r) \right], \quad (2)$$

in any coordinate system, where $r_< = \min(|r_s|, |r_r|)$, $r_> = \max(|r_s|, |r_r|)$. $P_0 = \omega\rho_0 q/(4\pi)$, ω being the angular frequency, ρ_0 the density of the medium, q the point source strength in unit of m^3/s, $k = \omega/c_0$ the wave number, and c_0 the speed of sound. $j_l(x)$ is the *spherical Bessel function* of order l and $h_l(x) = j_l(x) - i\, n_l(x)$ is the *spherical Hankel function* of order l, where $n_l(x)$ is the *spherical Neumann function* of order l. The spherical harmonics are defined as

$$Y_{lm}(\theta, \phi) = \sqrt{\frac{2l+1}{4\pi} \frac{(l-m)!}{(l+m)!}} P_l^m(\cos\theta) \mathrm{e}^{\mathrm{i}m\phi}, \quad (3)$$

where $P_l^m(\cos\theta)$ is the associated Legendre function of degree l and order m evaluated at $\cos\theta$[14].

The scattered field from Sphere 1 in the presence of Sphere 2 is better expressed in the coordinate system O_1 as

$$p_{s_1}(\boldsymbol{r}_{1r}) = \sum_{l=0}^{\infty} \sum_{m=-l}^{l} C'_{lm} h_l(kr_{1r}) Y_{lm}(\theta_{1r}, \phi_{1r}), \quad (4)$$

and the scattered field from Sphere 2 in the presence of Sphere 1 is better expressed in the coordinate system O_2 as

$$p_{s_2}(\boldsymbol{r}_{2r}) = \sum_{l=0}^{\infty} \sum_{m=-l}^{l} D'_{lm} h_l(kr_{2r}) Y_{lm}(\theta_{2r}, \phi_{2r}), \quad (5)$$

where C'_{lm} and D'_{lm} are unknown scattering coefficients yet to be determined [14].

By using the identity $P_l^{-m}(\cos\theta) = (-1)^m P_l^m(\cos\theta) \cdot (l-m)!/(l+m)!$, equation (2) can be rewritten as

$$p_p(\boldsymbol{r}) = \sum_{l=0}^{\infty}\sum_{m=0}^{l}\Big\{A_{lm} j_l(kr_<) h_l(kr_>) P_l^m(\cos\theta_s) \cdot P_l^m(\cos\theta_r)\cos\left[m(\phi_r-\phi_s)\right]\Big\}, \quad (6)$$

where

$$A_{lm} = k P_0 \varepsilon_m \frac{(2l+1)}{4\pi}\frac{(l-m)!}{(l+m)!}, \quad (7)$$

with $\varepsilon_m = 1$ for $m = 0$ and $\varepsilon_m = 2$ for all other m.

Using $C'_{lm} = C_{lm} Y^*_{lm}(\theta_s, \phi_s)$ and $D'_{lm} = D_{lm} Y^*_{lm}(\theta_s, \phi_s)$ while repeating the algebra above, equations (4)–(5) can be rewritten as

$$p_{s_1}(\boldsymbol{r}_{1r}) = \sum_{l=0}^{\infty}\sum_{m=0}^{l}\Big\{C_{lm} h_l(kr_{1r}) P_l^m(\cos\theta_{1r}) \cdot P_l^m(\cos\theta_{1s})\cos\left[m(\phi_{1r}-\phi_{1s})\right]\Big\} \quad (8)$$

$$p_{s_2}(\boldsymbol{r}_{2r}) = \sum_{l=0}^{\infty}\sum_{m=0}^{l}\Big\{D_{lm} h_l(kr_{2r}) P_l^m(\cos\theta_{2r}) \cdot P_l^m(\cos\theta_{2s})\cos\left[m(\phi_{2r}-\phi_{2s})\right]\Big\}. \quad (9)$$

Equations (8)–(9) have now to be written in the same coordinate system. This can be achieved by using the forward and backward vertical translational addition theorem in the current specific coordinates [15, 16], which has

$$h_l(kr_2) P_l^m(\cos\theta_2) = \sum_{n=m}^{\infty} B_{mn}^{ml}(kd) j_n(kr_1) \cdot P_n^m(\cos\theta_1), \quad (10a)$$

$$h_l(kr_1) P_l^m(\cos\theta_1) = \sum_{n=m}^{\infty} F_{mn}^{ml}(kd) j_n(kr_2) \cdot P_n^m(\cos\theta_2), \quad (10b)$$

where d is the distance between the centre of the spheres and the forward and backward vertical translational coefficients are given by

$$F_{mn}^{ml}(kd) = (-1)^m(-i)^{n-l}(2n+1) \cdot \sum_{p=|l-n|}^{l+n}(i)^p g(m,l,-m,n,p) h_p(kd), \quad (11a)$$

$$B_{mn}^{ml}(kd) = (-1)^m(-i)^{n-l}(2n+1) \cdot \sum_{p=|l-n|}^{l+n}(-i)^p g(m,l,-m,n,p) h_p(kd), \quad (11b)$$

with $p = \{l+n,\ l+n-2, \cdots, |l-n|\}$, and the Gaunt coefficients are given by

$$g(m,l,-m,n,p) = (2p+1)\sqrt{\frac{(l+m)!(n-m)!}{(l-m)!(n+m)!}} \cdot \begin{pmatrix} l & n & p \\ 0 & 0 & 0 \end{pmatrix}\begin{pmatrix} l & n & p \\ m & -m & 0 \end{pmatrix}. \quad (12)$$

Note that $(\cdot)$ in equation (12) does not refer to a matrix but a Wigner 3-j symbol. More details on the Wigner 3-j symbol and a method to calculate their products efficiently can be found in the references [15, 16].

Substituting equations (6), (8), (9) and (10) in equation (1), applying the boundary condition $\mathrm{j}\rho\omega v_n(r) = -\partial p_t(\boldsymbol{r})/\partial r = 0$ at the surface of each rigid sphere in its own coordinate system, truncating the summations to a constant L, and using the orthonormality properties of the spherical harmonics to equate the coefficients of $P_l^m(\cos\theta_{i_R})\cos[m(\phi_{i_R}-\phi_{i_S})]$ to zero, the following coupled linear complex equations are obtained

$$\begin{cases} C_{lm} h_l'(ka) P_l^m(\cos\theta_{1s}) \\ \quad + \sum_{q=0}^{L} D_{qm} B_{ml}^{mq}(kd) j_l'(ka) P_q^m(\cos\theta_{2s}) = \\ \quad\quad -A_{lm} j_l'(ka) h_l(kr_{1s}) P_l^m(\cos\theta_{1s}), \\ \sum_{q=0}^{L} C_{qm} F_{ml}^{mq}(kd) j_l'(ka) P_q^m(\cos\theta_{1s}) \\ \quad + D_{lm} h_l'(ka) P_l^m(\cos\theta_{2s}) = \\ \quad\quad -A_{lm} j_l'(ka) h_l(kr_{2s}) P_l^m(\cos\theta_{2s}) \end{cases} \quad (13)$$

with $lm = \{(0,0)\ (1,0)\ (1,1)\ (l,0)\cdots(l,m)\cdots(L,L)\}$, which makes it possible to determine the $(L+1)(L+2)$ unknown coefficients C_{lm} and D_{lm}. The total sound field can then be calculated by substituting these coefficients back in equations (8)–(9), respectively in equation (1).

The problem of acoustic scattering by two rigid spheres has already been thoroughly studied [15, 17]. In this section the method that was used to resolve this problem is repeated while a further simplification (resulting in the equations (6)–(8)) is added, which reduce the number of unknown coefficients to be determined from $2(L+1)^2$ to $(L+1)(L+2)$. In these simulations we assumed $P_0 = 1$. Source and receiver are both placed in the same plane xz, so that the term $\cos[m(\phi_{i_R}-\phi_{i_S})]$ equals 1 if they are both in the same (positive or negative) region of the x axis or -1 otherwise. The truncation order used was $L = (\lceil ka \rceil + 10)$.

3. Simulation Results

In this section the results of simulations that were carried out with a crosstalk cancellation system with four point sources and two binaural receivers (equivalent to two listeners) are presented. The simulations were based on the two rigid sphere model presented in the last section. The alteration of the sound field due to the presence of the two scattering spheres is depicted in Figure 2. Instead of a constant pressure value throughout the whole frequency spectrum, as obtained with the free-field model, the pressure value obtained while using the new model fluctuates heavily throughout the spectrum. The presence of a second sphere also cancels out the symmetry effect observed while using the free-field model on Figure 2a.

When it comes to a one listener CTC, several different metrics such as condition number, channel separation level, and sweet spot size, among others, have been proposed and analyzed [4, 6]. In this paper the condition number of the transfer matrix is used to describe the robust performance of the CTC system, so that the results presented

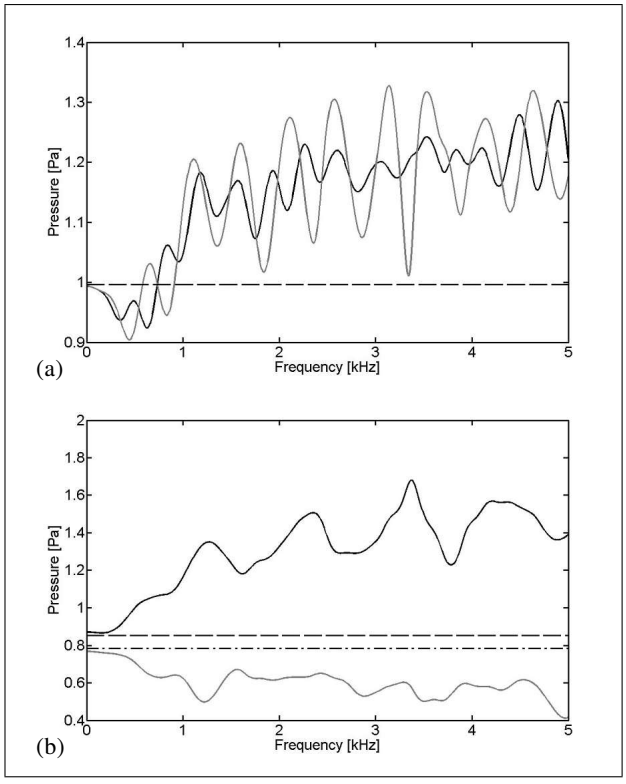

Figure 2. Pressure generated by a point source with $P_0 = 1$ located at $s = (1, 0, d/2)$ using the two discussed models. The spheres are centred at $(0, 0, d/2)$ and $(0, 0, -d/2)$. (a) The pressure is calculated at $r_1 = (0, 0, d/2 + a)$ and $r_2 = (0, 0, d/2 - a)$ with the free-field model (dotted line) and the two sphere model (dark solid line for r_1, light solid line for r_2). (b) The pressure is calculated at $r_3 = (0, 0, -d/2 + a)$ and $r_4 = (0, 0, -d/2 - a)$ with the free-field model (dashed line for r_3 and dot-dashed line for r_4) and the two sphere model (dark solid line for r_3, light solid line for r_4).

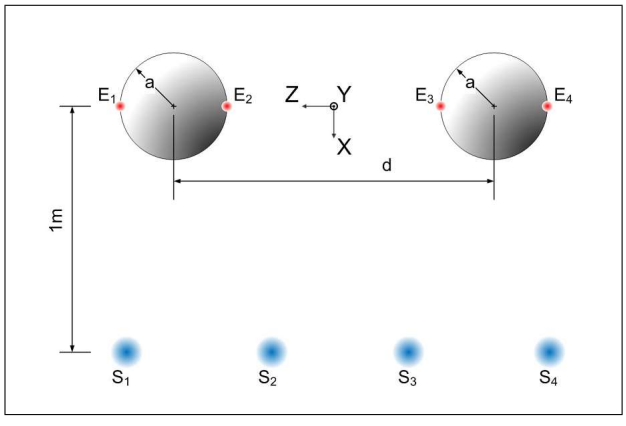

Figure 3. Example of configuration used for the simulation of the two listeners CTC system.

here can be compared with the analysis of a two listeners CTC carried out by Kim *et al*. The system's conditioning is obtained by creating, for each considered frequency in the range from 0 to 5 kHz, a four by four transfer matrix $\boldsymbol{C}(\omega)$ where each of its elements $\boldsymbol{C}_{rs}$ is a transfer function between the source s and the receiver r. Afterward

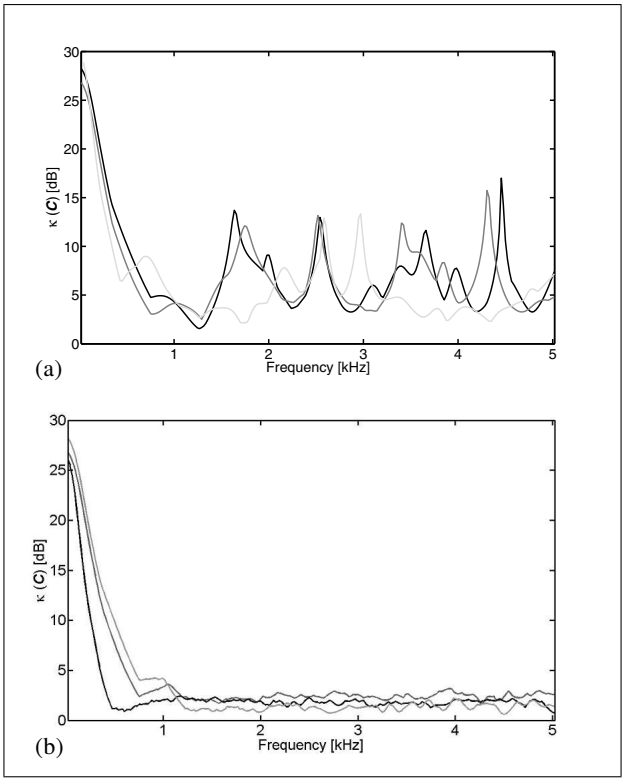

Figure 4. The behaviour of the condition number from the plant transfer matrix $\boldsymbol{C}(\omega)$ for three simulated models: the free-field model (light gray line) and the two rigid sphere model with linear source distribution (dark gray line), and the two rigid sphere model with circular source distribution (black line). (a) The source positions are chosen as to minimize the average of $\kappa(\boldsymbol{C}(\omega))$ over the entire frequency band. (b) The source positions are chosen as to minimize $\kappa(\boldsymbol{C}(\omega))$ in every frequency.

the condition number $\kappa(\boldsymbol{C}(\omega))$ of the plant transfer matrix was analyzed for all possible arrangements of the four sources. Two possible source distribution schemes, a linear and a circular distribution, were simulated. The results are discussed in the following sections.

3.1. Linear Distribution

The simulated geometry with the origin of the coordinate system between both spheres is depicted in Figure 3. The radii of the spheres were chosen to be $a = 0.09$ m and the distance between their centres was set to $d = 0.52$ m. The possible source locations are assumed to be at 0.05 m intervals within the range from -0.6 to 0.6 m along the line $(x = 1, y = 0)$ m. These distances where chosen as they have already been used by Kim *et al.* for their simulations [11].

When using only one source arrangement for the two person CTC system, it is necessary, as depicted in Figure 4a, to account for an elevated condition number at certain frequencies. Figure 4a shows the value of the condition number as a function of frequency for the source arrangement that minimizes the average of $\kappa(\boldsymbol{C}(\omega))$ over the entire frequency band – for the free-field model and the two sphere model with linear and circular source dis-

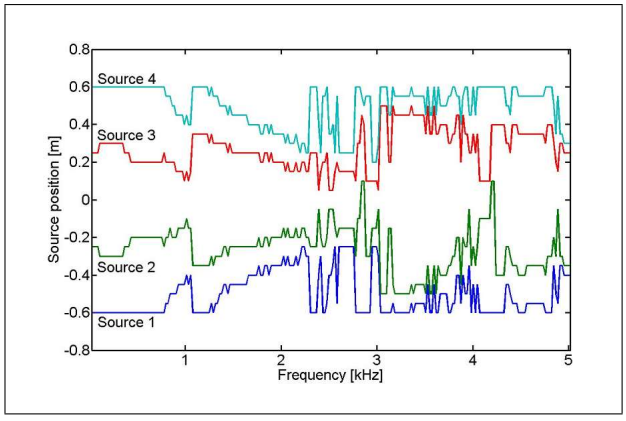

Figure 5. Position of the four point sources that gives the smallest condition number $\kappa(\boldsymbol{C}(\omega))$ at each frequency. Even though no symmetry was forced within the possible combinations, the distributions tend to be symmetric for the given receiver geometry.

tributione source arrangement that minimizes $\kappa(\boldsymbol{C}(\omega))$ for the free-field and rigid sphere models is the same and was created by placing the point sources at $z = (-0.6, -0.3, 0.3, 0.6)$. It is important to point out that other source arrangements not tested here might yield a better result. The peak present in both curves at the region of 2.5 kHz occurs due to the fact that the system is badly conditioned in this region, what is equivalent to say that the filter gains at that frequency are considerably high or that the generated sound field varies rapidly in space. This means that a movement of only 5 mm to the side would cause a variation bigger than 5 dB at the local sound pressure.

By choosing an appropriate source distribution for each frequency it is possible to keep $\kappa(\boldsymbol{C}(\omega))$ below 5 dB for frequencies higher than approximately 1 kHz in all three cases. The value of the smallest condition number found for each frequency can be seen in Figure 4b. The graphic suggests that the condition of a real CTC system might be better than that estimated with the free-field model for lower frequencies. The position that gives the smallest condition number for each frequency for the two rigid sphere model is presented at Figure 5. Note that even though no symmetry was forced for the source positioning, the source distribution is relatively symmetrical and in accordance with the symmetry of the receivers. Just as for the free-field model [11], each frequency requires a different source arrangement that leads to an impractical implementation since such a system would require a great number of loudspeakers positioned very closely to each other and very narrow band filters to split the channel to each of the loudspeaker arrangement.

The curves presented in Figure 4a are of great relevance when it comes to understanding why the results obtained with the newly presented model differ so little from the free-field model results. Even for a very simple and symmetrical transducers arrangement, the condition number calculated with the flat HRTFs provided by the free-field model is not well behaved and predictable as is the case

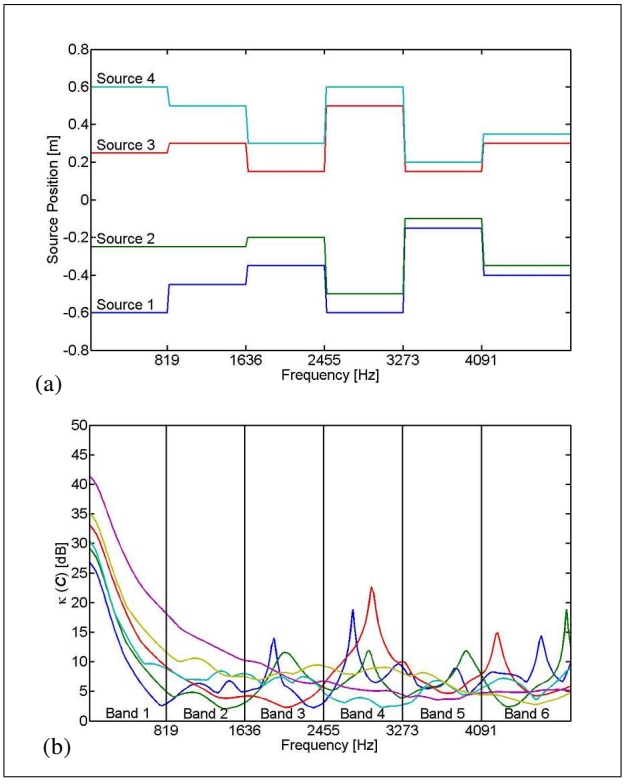

Figure 6. (a) The point source positions that minimize the average of $\kappa(\boldsymbol{C}(\omega))$ over each frequency band. (b) The behaviour of the condition number from the plant transfer matrix $\boldsymbol{C}(\omega)$ for the respective six source positions.

for the one listener CTC [7]. With that said, it is not to be expected that the HRTFs calculated with the two sphere model provide a condition number curve better behaved as the one obtained with the flat HRTFs of the previous model. Due to the fact that the condition number curves have no defined trends for both models, a considerable improvement of the systems description can not be noticed with the new two sphere model.

In search of a compromise between the number of required sources and the value of the condition number Kim *et al.* [11] defined six frequency bands and found for each band the source arrangement that minimizes the average condition number within each band. This procedure was repeated for the two sphere model and the results are presented in Figure 6. In comparison with the results obtained for the free-field model [11], an improvement of around 5 dB can be noticed at the two higher frequency bands. This improvement can be explained by the fact that the scattering from a sphere becomes very directional for $ka > 5$ (in this case $f > 3$ kHz) [14] and if one sphere is positioned in the shadow region of the other sphere, the systems coupling is reduced and thus the condition number decreases as well.

3.2. Circular Distribution

In another attempt to improve the conditioning of the two listener CTC filters, a new source positioning was simulated with the possible source locations distributed over a

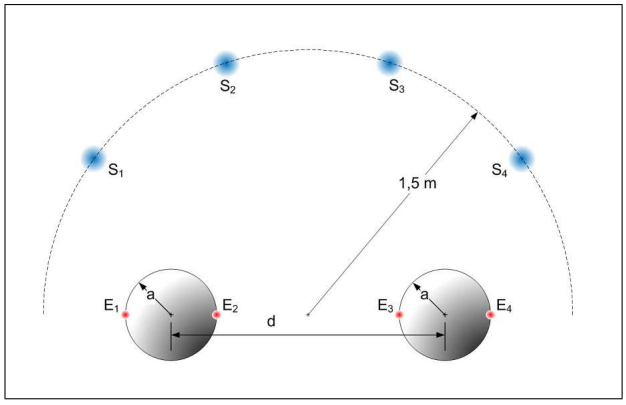

Figure 7. Two listeners CTC system model with possible source positions placed over a 1.5 m semi-circle. The dotted line starts at −90° on the left and ends at 90° on the right.

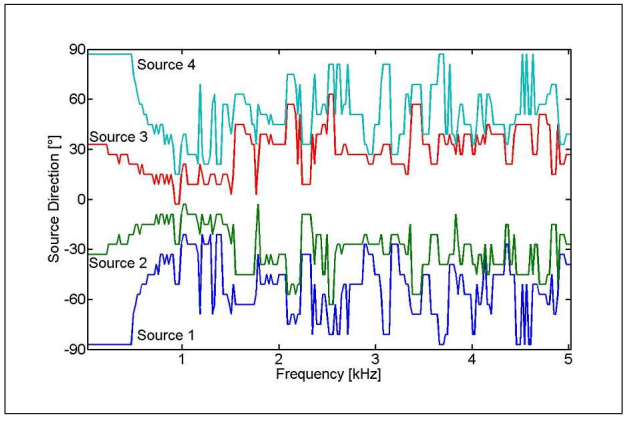

Figure 8. The point source positions, given in angle over a 1.5 m radius semi-circle, that minimizes $\overline{\kappa(\boldsymbol{C}(\omega))}$ in each frequency. Note that no symmetry was forced.

semi-circle with a radius of 1.5 m, as shown in Figure 7. Once again, it was not possible to find a single source arrangement that yield a low condition number throughout the whole frequency band, as can be seen in Figure 4a. For frequencies higher than 1 kHz no significant change can be noted on the minimal condition number. For lower frequencies a considerable improvement in terms of the relation to the other two models is noticed. One must be cautious to relate this improvement in lower frequencies directly to the new source geometry, since the distance between the sources and the receivers is now different. However, simulations with semi-circles with smaller radii maintained this trend confirming the improvement in middle frequencies while using circularly distributed sources.

It can be seen in Figure 8 that the source position presents a clear trend in the region between 500 Hz and 1 kHz. That means that for every frequency in this range a distinct and well defined source arrangement that minimizes the condition number of the transfer matrix exists. This fact prevents band optimized systems, like the one proposed in the last section, from reproducing such an improvement in middle frequencies. The behaviour of the circularly and linearly distributed system is similar for higher frequencies. It can thus be observed that there is no practical difference between the two source distribution schemes for a band optimized system.

A full circular distribution was not tested because of the symmetric nature of this problem. It is also important to mention that a symmetrical displacement of the sources, as if they were positioned on the vertices of a square centered on the origin is the worst possible case in terms of the robustness of the crosstalk cancellation if the two listeners are symmetrically positioned around the origin, since this situations results in a linearly dependent transfer matrix that has no exact inverse.

4. Conclusion

The objective of this paper was to expand the simulation models of multi-listeners *crosstalk cancellation* systems by taking into consideration the diffraction effect of the listeners head simulating them as two rigid spheres. A widely known method for calculating the pressure field of two scattering rigid sphere was for the first time used for modelling a two listener CTC system and the condition number of the transfer matrix calculated with this method was analyzed. It was verified that it is possible to find a source arrangement that minimizes the condition number of the transfer matrix for every frequency in the middle and high frequency bands. However, as the ideal position varies significantly for neighbouring frequencies, a practical implementation of such systems is difficult. A band optimized system was also simulated. Such a system reduces on the one hand the number of sources needed but on the other hand results in higher condition number values throughout the spanned frequency range. The results obtained with the sources distributed circularly instead of linearly in front of the listeners showed a potential improvement of the system in the middle frequency range. The practical application of this system, however, remains difficult.

Acknowledgements

We would like to thank Prof. Dr. M. Vorländer for supporting this work. The first author is a scholarship holder from CNPq, Conselho Nacional de Desenvolvimento Científico e Tecnológico - Brazil. The second author is supported by the Alexander von Humboldt Foundation and Project 10674068 of NSFC and NCET.

References

[1] M. Vorländer: Auralization. Springer-Verlag, 2008.

[2] O. Kirkeby, P. A. Nelson, H. Hamada: The "stereo dipole" - a virtual source imaging system using two closely spaced loudspeakers. J. Audio Eng. Soc. **46** (1998) 387–395.

[3] W. G. Gardner: 3-d audio using loudspeakers. Massachusetts Institute of Technology, 1997.

[4] T. Lentz: Binaural technology for virtual reality. Institut für Technische Akustik, RWTH-Aachen, 2007.

[5] D. B. Ward, G. W. Elko: Effect of loudspeaker position on the robustness of acoustic crosstalk cancellation. IEEE Signal. Proc. Let. **6** (1999) 106–108.

[6] M. R. Bai, C.-C. Lee: Objective and subjective analysis of effects of listening angle on crosstalk cancellation in spatial

sound reproduction. J. Acoust. Soc. Am. **120** (2006) 1976–1989.

[7] P. A. Nelson, J. F. W. Rose: The time domain response of some systems for sound reproduction. J. Sound Vib. **296** (2006) 461–493.

[8] D. Malham: Homogeneous and nonhomogeneous surround sound systems. AES UK "Second Century of Audio" Conference, London, 1999.

[9] J. Daniel, S. Moreau, R. Nicol: Further investigations of high-order ambisonics and wavefield synthesis for holophonic sound imaging. 114th AES Convention, Amsterdam, The Netherlands, 2003.

[10] J. Bauck, D. H. Cooper: Generalized transaural stereo and applications. J. Audio Eng. Soc. **44** (1996) 683–705.

[11] Y. Kim, O. Deille, P. A. Nelson: Crosstalk cancellation in virtual acoustic imaging systems for multiple listeners. J. Sound Vib. **297** (2006) 251–266.

[12] P. A. Nelson, Y. Kahana: Spherical harmonics, singular-value decomposition and the head-related transfer function. J. Sound Vib. **239** (2001) 607–637.

[13] Z. Lin, J. Lu, C. Shen, X. Qiu, B. Xu: Active control of radiation from a piston set in a rigid sphere. J. Acoust. Soc. Am. **115** (2004) 2954–2963.

[14] E. G. Williams: Fourier acoustics: Sound radiation and nearfield acoustical holography. Academic Press, 1999.

[15] G. C. Gaunaurd, H. Huang, H. C. Strifors: Acoustic scattering by a pair of spheres. J. Acoust. Soc. Am. **98** (1995) 495–507.

[16] K. M. Li, W. K. Lui, G. H. Frommer: The diffraction of sound by an impedance sphere in the vicinity of a ground surface. J. Acoust. Soc. Am. **115** (2004) 42–56.

[17] J. H. Wu, A. Q. Liu, H. L. Chen, T. N. Chen: Multiple scattering of a spherical acoustic wave from fluid spheres. J. Sound Vib. **290** (2006) 17–33.